J Med Syst (2015) 39: 95
DOI 10.1007/s10916-015-0279-2

SYSTEMS-LEVEL QUALITY IMPROVEMENT

A Study on the Optimal Positions of ECG Electrodes in a Garment for the Design of ECG-Monitoring Clothing for Male

Hakyung Cho[1] · **Joo Hyeon Lee**[2]

Received: 6 April 2014 / Accepted: 1 June 2015 / Published online: 8 August 2015

Abstract Smart clothing is a sort of wearable device used for ubiquitous health monitoring. It provides comfort and efficiency in vital sign measurements and has been studied and developed in various types of monitoring platforms such as T-shirt and sports bra. However, despite these previous approaches, smart clothing for electrocardiography (ECG) monitoring has encountered a serious shortcoming relevant to motion artifacts caused by wearer movement. In effect, motion artifacts are one of the major problems in practical implementation of most wearable health-monitoring devices. In the ECG measurements collected by a garment, motion artifacts are usually caused by improper location of the electrode, leading to lack of contact between the electrode and skin with body motion. The aim of this study was to suggest a design for ECG–monitoring clothing contributing to reduction of motion artifacts. Based on the clothing science theory, it was assumed in this study that the stability of the electrode in a dynamic state differed depending on the electrode location in an ECG-monitoring garment. Founded on this assumption, effects of 56 electrode positions were determined by sectioning the surface of the garment into grids with 6 cm intervals in the front and back of the bodice. In order to determine the optimal locations of the ECG electrodes from the 56 positions, ECG measurements were collected from 10 participants at every electrode position in the garment while the wearer was in motion. The electrode locations indicating both an ECG measurement rate higher than 80.0 % and a large amplitude during motion were selected as the optimal electrode locations. The results of this analysis show four electrode locations with consistently higher ECG measurement rates and larger amplitudes amongst the 56 locations. These four locations were abstracted to be least affected by wearer movement in this research. Based on this result, a design of the garment-formed ECG monitoring platform reflecting the optimal positions of the electrode was suggested.

Keywords Sensor positions · ECG monitoring · ECG electrode · Motion artifact · Optimal location of electrode · Wearable platform · Smart clothing

This article is part of the Topical Collection on *Systems-Level Quality Improvement*

✉ Joo Hyeon Lee
ljhyeon@yonsei.ac.kr

Hakyung Cho
hkcho1010@gmail.com

[1] BLACKYAK Co. Ltd., Seoul, Republic of Korea

[2] Department of Clothing and Textile, Yonsei University, Seoul, Republic of Korea

Introduction

Due to increasing health concerns, a wellness-focused lifestyle and an aging society, the need for supporting devices for ubiquitous health care and wellness has recently increased [1, 5, 10, 19, 22]. Along with this trend, portable or wearable devices and techniques for ubiquitous vital sign measurement have recently been introduced in the research fields of health monitoring and healthcare systems for patients and elderly people [11, 16, 18, 19]. However, the current devices for vital sign monitoring are too clumsy and uncomfortable for long-term or daily use [13].

Smart clothing for health promotion enabling the continuous monitoring of vital signs is considered an intelligent medical monitoring device, as it provides real-time feedback to the patient on the basis of continuous measurements [17]. Smart

clothing for vital sign monitoring has been studied and developed in various applications of clothing for monitoring electrocardiography (ECG), respiration, posture, etc. [2, 4, 8, 9, 14, 15, 23]. However, smart clothing for vital sign monitoring has had the serious weakness of being affected by motion artifacts. In effect, the motion artifact is one of the major problems in practical implementations of most wearable health monitoring devices.

In contact-type ECG monitoring clothing, the motion artifact has been known to be caused by three major factors. The first factor, the lack of contact between the human body and the electrode, is attributed to the improper fit of the garment to the human body. The second factor is the improper location of the electrode on a garment leading to shifting of the electrode position in the garment caused by the wearer's motion. The last factor leads to electrical errors, such as errors in the apparatus arrangement. Therefore, it is necessary to find solutions to minimize motion artifacts in order to improve the accuracy of the ECG measured through the clothing.

Among the three major factors above, the first one, the lack of contact between the human body and the electrode, has been improved by some useful suggestions for the clothing and electrode designs in previous developments [3, 20, 21].

For the second factor, however, there has not been plentiful research on the motion artifacts which are caused by the interaction between the human body and the electrodes such as the stability of the electrode position being affected by body movement [1, 7, 12].

Therefore, it is essential to observe and analyze the interaction between the wearer's body and the electrodes laid out on the clothing surface during the wearer's movement in order to find efficient ways to minimize motion artifacts in ECG monitoring clothing.

For this, influential factors in the interaction between the human body and the electrode locations on ECG-monitoring clothing were analyzed empirically in this study. Based on the result of the empirical analysis, the optimal locations of the ECG electrode for the garment were extracted. A design for the garment-formed ECG monitoring platform reflecting the optimal positions of the electrodes was recommended in the final part of this study.

The research method

In order to fulfill the purpose of this study, the experiment and the devices were prepared as follows:

Design of the experimental garment

A piece of the experimental garment was designed in the form of a tight-fitted sleeveless top, made of stretchy fabric composed of 92 % polyester and 8 % polyurethane.

To determine the optimal electrode location, the surface of the garment was sectioned into grids with 6 cm intervals starting from the center-top in the front and back of the bodice. The grid-sectioned top, including a total of 56 positions for ECG electrodes with 6 cm intervals, was produced (Fig. 1).

A dry ECG electrode comprised of nickel, was devised in the form of a snap button set with a 12 mm diameter and applied to the experimental garment, as shown in Fig. 2. Each dry electrode was composed of two parts: on the back and front sides. For attachment to the garment, the electrodes were laid out to sandwich the fabric of the garment between the two sides and then to interlock with a penetrating needle from the back to the center-front, as shown in Fig. 2. The back side contacting the wearer's skin was designed to press gently against the skin, while the front side was designed to allow a connection between the electrode and the wires from the ECG equipment. To maintain stable contact between the electrode and the wearer's skin, a pressure of 40 gf/cm^2, which indicated 'tightly-fitting but still comfortable' according to clothing science theory, was applied to the experiment garment.

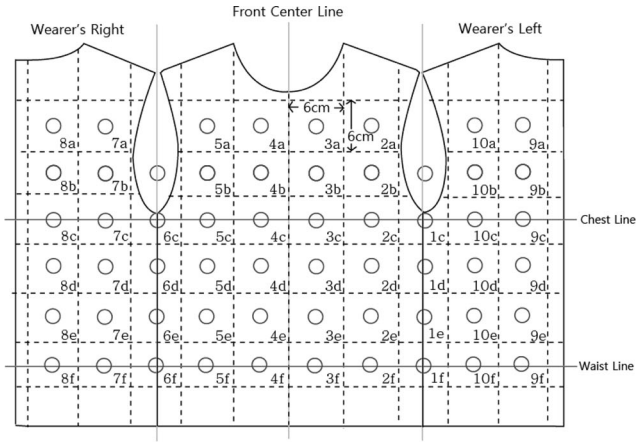

a) grid-sectioned top design.

b) grid-sectioned top design on clothing.

Fig. 1 The grid-sectioned top including 56 electrode positions. **a** grid-sectioned top design. **b** grid-sectioned top design on clothing

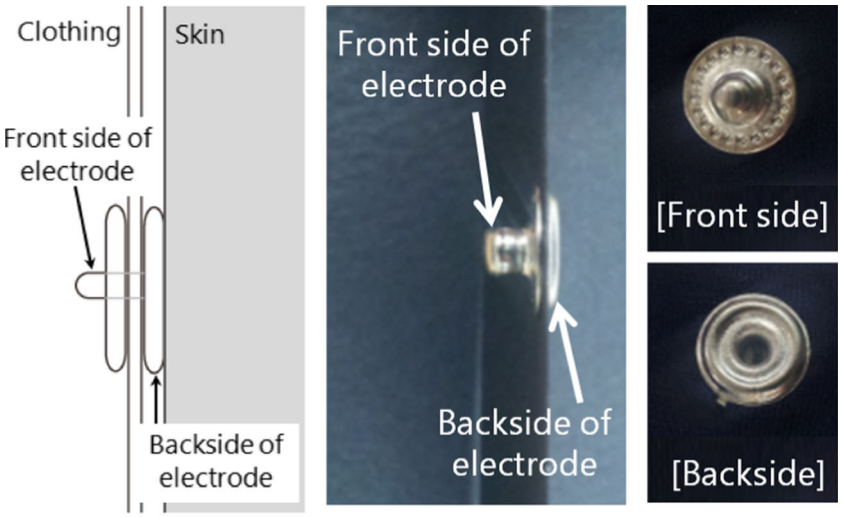

a)Basic principal of dry electrode

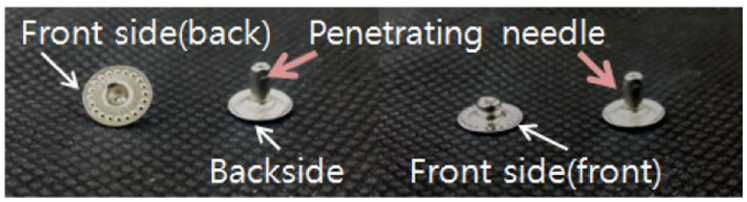

b)Penetrating needle for connection of both sides.

Fig. 2 The dry ECG electrode attached to the experimental garment. **a** Basic principal of dry electrode. **b** Penetrating needle for connection of both sides

Sensor characterization

As the focus of this research was proper or improper locations of the electrode on a garment, one of the three factors influencing motion artifacts in contact-type ECG monitoring clothing, a metal electrode was devised for use in this study. The reason for adopting a button-type metal electrode instead of a textile one was to assess the appropriateness of the electrode locations on the garment surface without any intervening effect from the electrical difference between textile and metal materials used for the electrode.

In order to assess the characteristics of the dry electrode in this study, the impedance of the electrode was measured using an equivalent circuit model (Fig. 3). An Ag/AgCl electrode (3 M, USA) was used as the reference electrode.

For the measurement of the input impedance of the dry electrode, the principle presented in Fig. 4 was applied. The impedance of [a–b] in Fig. 4 was obtained by equation (1), the impedance of [b–c] was obtained by equation (2), and the impedance of [a–c] was obtained by equation (3). If the skin-electrode impedance and the internal resistance are assumed to be identical, these equations can be simplified to equation (4). Accordingly, the target impedance, 'Zx', and the phase can finally be calculated by equation (5).

As the characteristics of the electrode significantly changed according to the level of external pressure, a pressure sensor (IESF-R-5L) was used to maintain an equivalent pressure of 40 gf/cm^2 on every electrode.

Precision LCR meter 4284A (20 Hz~1 MHz, Hewlett Packard) equipment was used to measure the impedance and electrical phase in each electrode position. Efficient observation of the characteristic changes in the vital sign band was

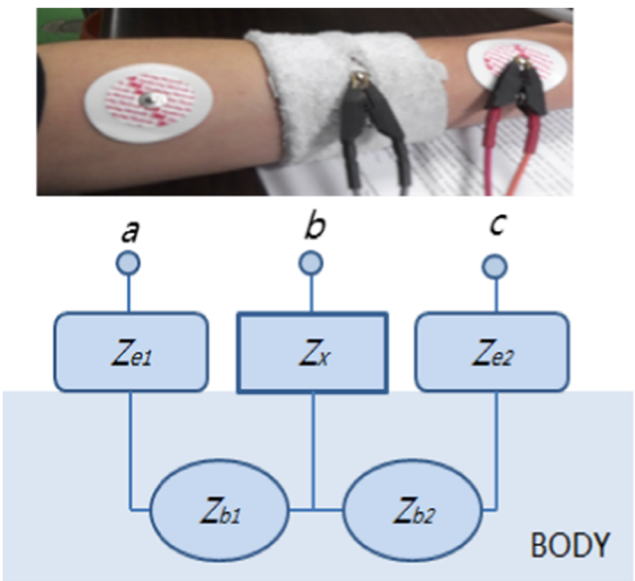

Fig. 3 The principles of the impedance measurement

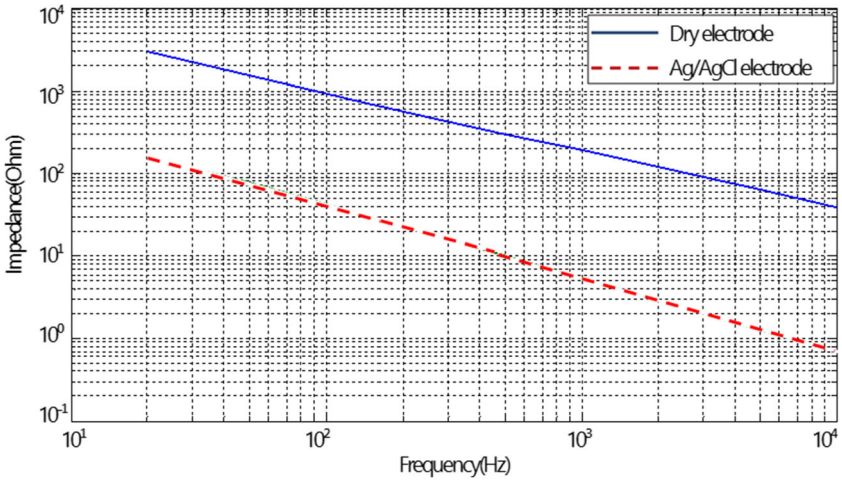

Fig. 4 The input impedance of the dry electrode

possible since the measurements could be executed at a low frequency band.

As shown in Fig. 4, the measured input impedance of the devised dry electrode has a similar tendency to that of the Ag/AgCl electrode in clinical measurements.

Motion protocols

In this study, the ECG was measured through the dry electrodes attached to the experimental garment while the wearer was in motion according to the directed motion protocols.

Nine motions were selected as representative of movements made during daily life based on the *activities of daily living* (ADL) scale and the *instrumental activities of daily living* (IADL) scale [11] and adopted as the motion protocols for the experiment.

As shown in Fig. 5, there are nine motion protocols including arm motions on both sides in the frontal, sagittal and horizontal plane directions, and three bodice motions: forward flexion, backward flexion and rotation of the spine.

Participants

This study recruited only male participants in order to evaluate the pure appropriateness of the electrode positions by limiting the intervening effect caused by differences in body curvature. Ten male participants aged between 22 and 27 years with a relatively normal amount of body curves were sampled for this experiment. Their average height was 173.1 cm (SD=2.38). The average chest circumference was 95.7 cm (SD=3.10) and the waist circumference was 85.7 cm (SD=2.20) (Table 1).

The experimental method

The following experiment was designed to determine the optimal locations of the electrode on the experimental garment that would be the least affected by the wearer's motion.

In each set of tasks, a participant wearing the experimental garment began in the upright posture, executed the nine motion protocols, and returned to the upright posture. Fifty-six task sets of the experimental motions were repeated three times with 10-s intervals. For each electrode, a total of 270 measurements (nine motions repeated three times by 10 participants) were performed (Fig. 6).

The method of ECG measurement provided by the America Health Association (AHA) was applied to the acquisition of the reference signal from every participant. On the basis of the AHA exercise standards for testing and training [6], the reference signal was measured by the three lead systems. On

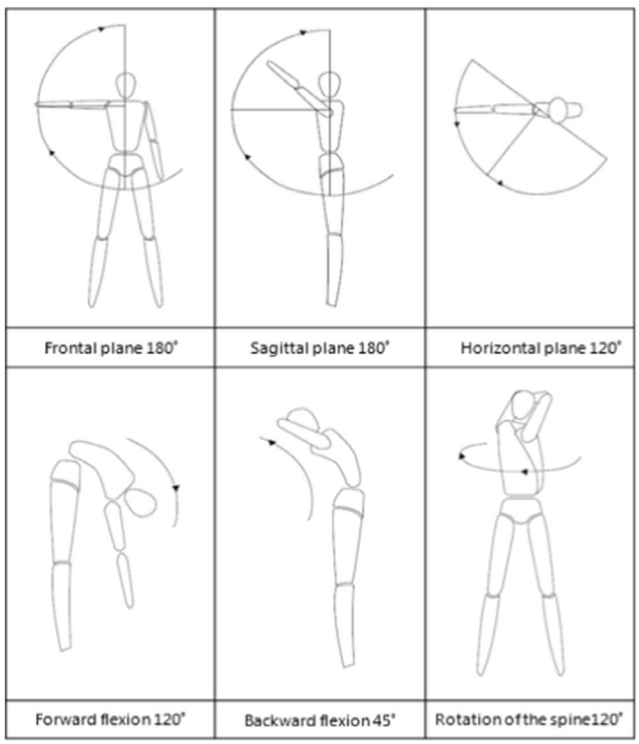

Fig. 5 The motion protocols for the experiment

Table 1 Characteristics of participants

	Gen	Age	Height(cm)	Bust (cm)	Waist(cm)	Skin type
P1	male	23	172	96	84	Less hairy
P2	male	24	170.5	95	85.2	Less hairy
P3	male	22	171	98	89.3	Less hairy
P4	male	26	173	98.2	85.2	Less hairy
P5	male	26	177	96.4	84.4	Less hairy
P6	male	27	176	98.2	87.4	Less hairy
P7	male	25	172	92.3	84.3	Less hairy
P8	male	25	175	98	89.4	Less hairy
P9	male	24	174	93.5	85.2	Less hairy
P10	male	25	170	92	83.1	Less hairy

the other hand, the targeted ECG signal was measured through the electrodes on the experimental garment, line by line (1~10 lines), for every participant (Fig. 7). To obtain the measurement rate of the targeted signal, the experimental ECG signal and the reference ECG signal were measured simultaneously for every participant and compared. The ECG signal acquired through the electrodes on the experimental garment was measured by BIOPAC® MP150 and ECG100C.

Evaluation method

The criteria to determine the optimal locations of the ECG electrodes were as follows:

Considering the motion artifacts caused by the wearer's movement, a measurement rate higher than 80.0 % was defined as a 'high measurement rate' in this study. The electrode locations showing a high measurement rate of the ECG during the motions were selected first in every participant's case. The measurement rate was calculated based on the number of the detected R-peaks counted which were matched with those in the reference signal obtained simultaneously (Fig. 8(a)).

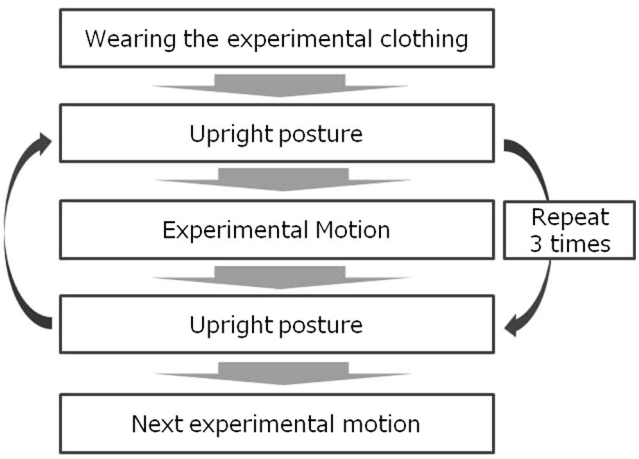

Fig. 6 The process of the experiment

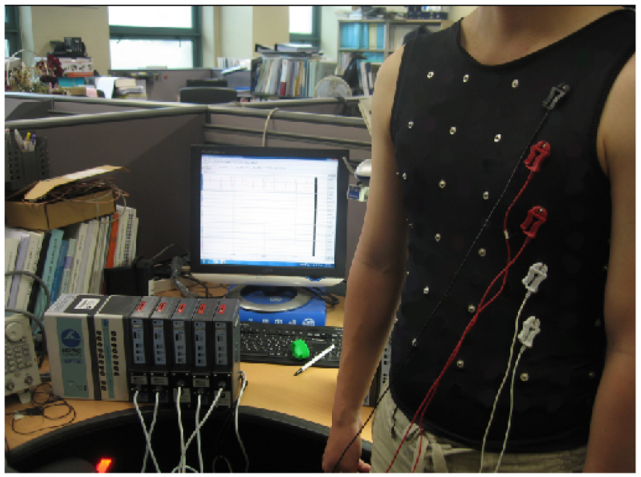

Fig. 7 The experimental method. **a** Principle of the measurement rate and amplitude value. **b** Distribution of measurement rate in garment. (*Blue-colored numbers* above the dots, indicate the large amplitude values obtained at the corresponding electrode locations)

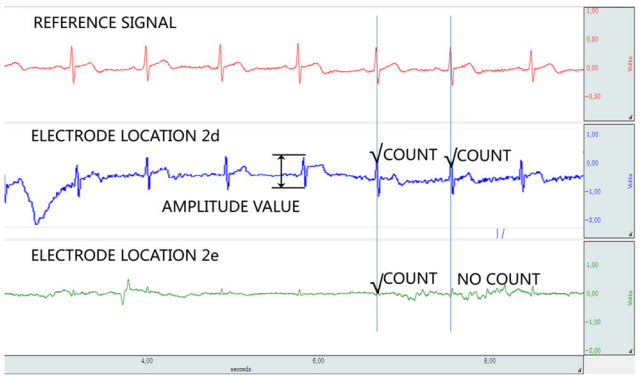

a) Principle of the measurement rate and amplitude value.

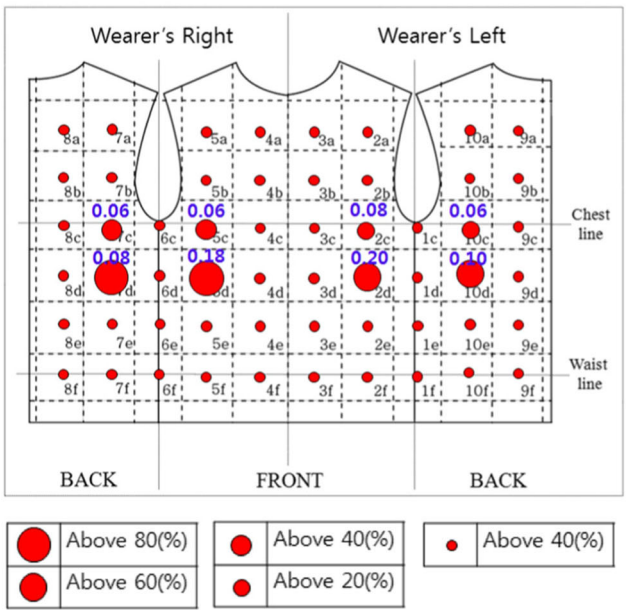

b) Distribution of measurement rate in garment.

Fig. 8 Conceptual diagram of evaluation method

Measurement rate was classified into the following five levels: 0~20, 20~40, 40~60, 60~80 and 80~100 %. Thus, 'a measurement rate higher than 80.0 %' means that more than 80.0 % of the detected R-peaks obtained through the devised electrode matched those in from the reference Ag/AgCl electrode. The resulting measurement rates were visually illustrated with dots of five different sizes, differing in 20 % intervals, as shown in Fig. 8(b). The largest amplitude among the detected measurement signals was defined as 'the large amplitude value' in this study. The blue numbers above the dots in Figs. 8 and 9 indicate the large amplitude values of voltage obtained at the corresponding electrode locations. Among the initially chosen electrode positions of each participant showing high ECG measurement rates, the electrode locations also showing a large ECG amplitude were classified as 'stable locations'.

The significance of the mean values of the measurement rate and the signal amplitude were verified by the Wilcoxon signed-rank test at the significance level of $p=0.05$. Based on the synthesized results across all the subjects, the electrode locations indicating both the high measurement rate and the large amplitude were selected as the optimal electrode locations.

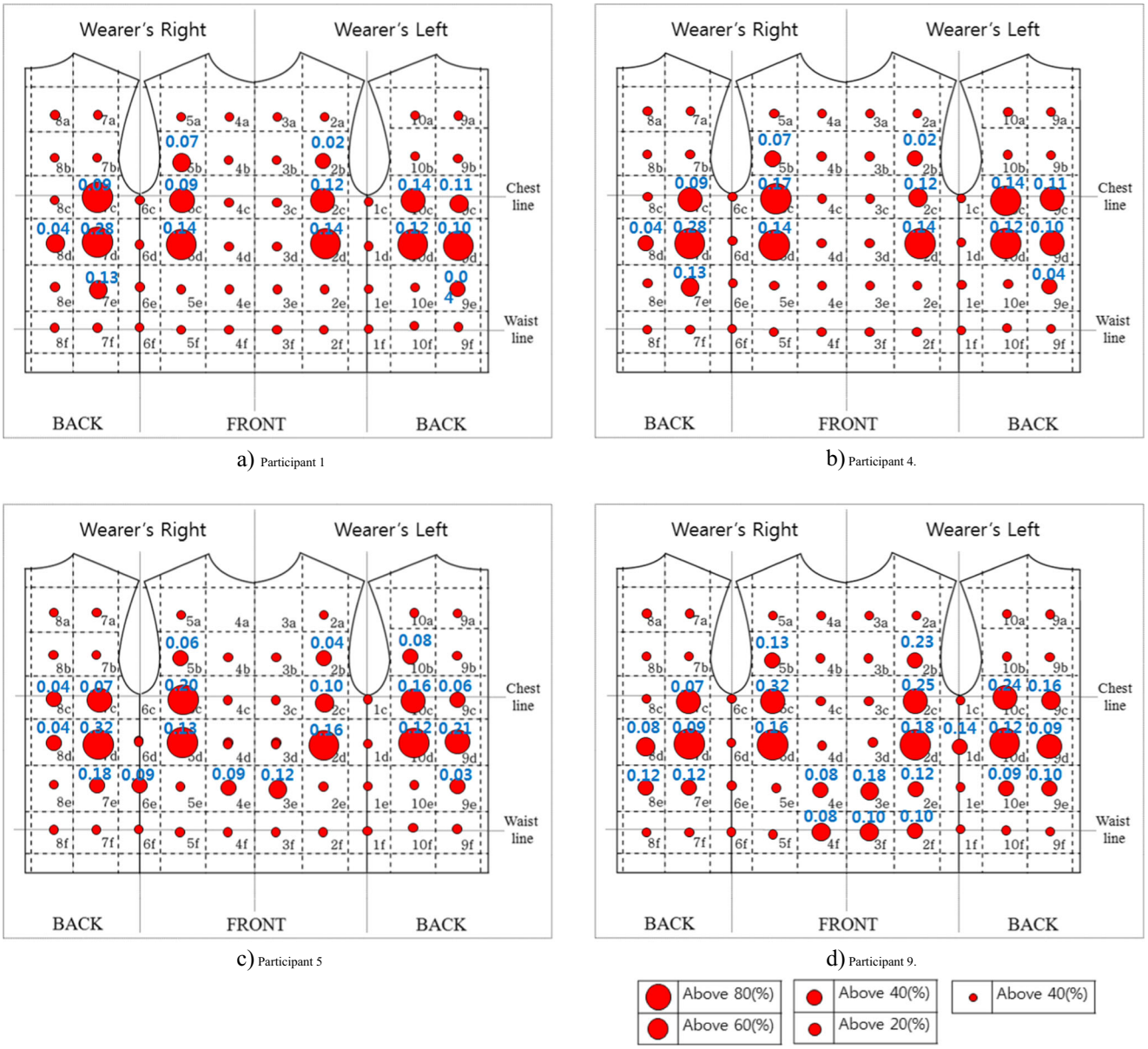

Fig. 9 Average values of the measurement rate and the amplitude of the experimental ECG. **a** Participant 1. **b** Participant 4. **c** Participant 5. **d** Participant 9. (*Blue-colored numbers* above the dots, indicate the large amplitude values obtained at the corresponding electrode locations)

Results and discussion

The measurement rate and amplitude of ECG

In the case of the right arm motion of participant 1 (Fig. 9(a) and Table 2(a)), high measurement rates from 83.0 to 97.7 % were obtained (87.0 % at electrode location 2d, 83.0 % at 5d, 95.7 % at 9d, and 97.7 % at 10c and 10d). In the left arm motion, high measurement rates were observed at 2d (84.7 %), 5d (92.3 %), 7c (86.7 %), 7d (100.0 %), 9d (82.7 %) and 10d (85.3 %). In the bodice motions, a high measurement is observed at electrode locations 5c (89.3 %), 5d (89.0 %), 7d (88.7 %) and 10d (83.3 %). In consideration of the averaged values of the measurement rates and amplitude across the nine motions, the electrode positions showing high measurement rates with a large amplitude were 2d (80.4 % and 0.14 V), 5d (88.3 %, 0.14 V), 7d (86.1 %, 0.28 V) and 10d (87.4 %, 0.12 V), in participant 1.

In participant 2, high measurement rates were observed at 5d (89.7 %) and 7d (87.0 %) in the right arm motions. High measurement rates were observed at electrode locations 5d (100.0 %) and 7d (100 %) in the left arm motions. In the bodice motions, high measurement rates were obtained at 5d (95.7 %) and 7d (83.7 %). The measurement rates in 2d and 10d were severely influenced by the arm motions on the frontal plane, as well as the backward flexion of the bodice. The average measurement rate and large amplitude value in all motions appeared to be high at 5d (95.3 %, 0.18 V) and 7d (88.6 %, 0.08 V). Accordingly, 5d and 7d were derived as the stable electrode locations in participant 2.

In participant 3, some relatively high measurement rates and amplitude values were obtained on lanes d~f when compared with the results from the other participants. Since participant 3 had a somatotype with a protruding abdomen, the experimental clothing was more tightly fitted to his body in the abdominal region. It was inferred that the relatively high measurement rates and amplitudes in these regions were attributed to the minimal shifting of the electrode positions in lanes d~f during the motions due to this tight fitting in the abdomen part. As a result, for the right arm motions, there were high measurement rates including 100.0 % at 1d, 100.0 % at 2c, 100.0 % at 2d, 94.0 % at 2e, 98.0 % at 2f, 98.0 % at 3d, 96.3 % at 3f, 87.0 % at 3f, 95.7 % at 5d, 100.0 % at 7d, 86.7 % at 8d, 98.0 % at 10d, 96.3 % at 10e and 91.3 % at 10 f. In the left arm motions, high measurement rates were also observed: 88.3 % at 1d, 91.3 % at 2e, 89.7 % at 2f, 94.0 % at 3e, 86.3 % at 4e, 88.3 % at 4f, 85.3 % at 5e, 80.7 % at 5d, 100.0 % at 7d and 84.7 % at 10d. In the bodice motions, high measurement rates were also observed: 81.3 % at 2d, 80.0 % at 5c, 94.3 % at 5d, 89.0 % at 7d and 84.0 % at 10d. The average measurement rate and large amplitude value in all motions appeared to be high at 2c (80.7 %, 0.37 V), 2d

Table 2 The higher measurement rates in the significant locations of electrode across the participants

Participant	Electrode location	1	2	3	4	5	6	7	8	9	10
1	c	0.0 %	60.5 %	0.0 %	1.2 %	77.6 %	1.0 %	62.7 %	7.2 %	48.5 %	66.4 %
	d	0.0 %	80.4 %	0.0 %	5.0 %	88.3 %	4.7 %	86.1 %	46.3 %	78.3 %	87.4 %
2	c	0.0 %	37.5 %	1.7 %	2.8 %	55.2 %	0.0 %	49.5 %	0.0 %	3.0 %	16.5 %
	d	0.0 %	75.0 %	0.0 %	0.5 %	95.3 %	0.0 %	88.6 %	2.3 %	0.0 %	69.3 %
3	c	0.0 %	80.7 %	31.7 %	21.3 %	78.6 %	3.5 %	34.3 %	6.5 %	36.2 %	76.5 %
	d	47.1 %	88.5 %	49.3 %	41.9 %	91.3 %	3.7 %	94.5 %	58.7 %	57.2 %	87.7 %
	e	50.1 %	83.9 %	82.0 %	61.1 %	48.4 %	24.7 %	28.6 %	15.6 %	32.6 %	33.4 %
4	c	0.0 %	57.3 %	0.6 %	1.2 %	83.0 %	1.0 %	76.1 %	7.3 %	69.3 %	86.8 %
	d	0.0 %	80.4 %	0.6 %	5.0 %	84.6 %	4.7 %	87.3 %	38.8 %	75.0 %	86.8 %
5	c	0.0 %	49.8 %	8.7 %	6.3 %	81.4 %	0.0 %	71.8 %	15.3 %	58.2 %	77.2 %
	d	0.0 %	80.5 %	13.4 %	9.8 %	83.0 %	8.0 %	86.5 %	37.0 %	69.8 %	80.4 %
6	c	12.6 %	64.9 %	0.0 %	7.8 %	85.4 %	4.0 %	78.2 %	26.6 %	67.2 %	91.8 %
	d	41.0 %	93.3 %	1.8 %	16.4 %	89.8 %	34.3 %	84.4 %	49.7 %	69.4 %	80.2 %
7	c	2.3 %	66.4 %	0.0 %	1.2 %	80.9 %	0.0 %	78.3 %	6.4 %	74.3 %	86.8 %
	d	43.0 %	89.9 %	0.0 %	10.8 %	83.9 %	1.0 %	82.7 %	34.8 %	56.8 %	80.0 %
8	c	0.0 %	48.3 %	7.0 %	4.2 %	81.6 %	1.3 %	82.0 %	6.8 %	55.8 %	80.6 %
	d	1.0 %	82.3 %	5.5 %	8.3 %	86.6 %	7.6 %	84.3 %	32.7 %	72.0 %	81.0 %
9	c	10.6 %	49.0 %	11.3 %	5.7 %	73.5 %	4.4 %	75.1 %	6.3 %	40.6 %	60.9 %
	d	21.2 %	86.3 %	9.1 %	14.4 %	85.8 %	5.9 %	84.6 %	33.5 %	62.0 %	80.5 %
10	c	0.0 %	48.3 %	7.0 %	4.2 %	81.6 %	1.3 %	82.0 %	6.8 %	55.8 %	80.6 %
	d	1.0 %	82.3 %	5.5 %	8.3 %	86.6 %	7.6 %	84.3 %	32.7 %	72.0 %	81.0 %

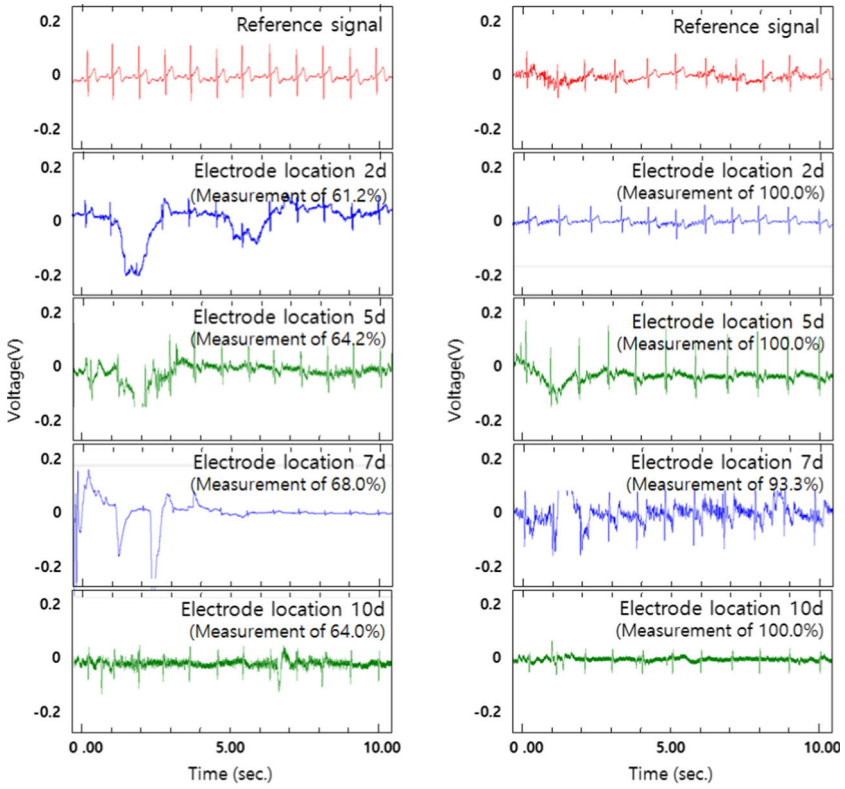

a)Frontal plane (R)

b)Sagittal plane (R)

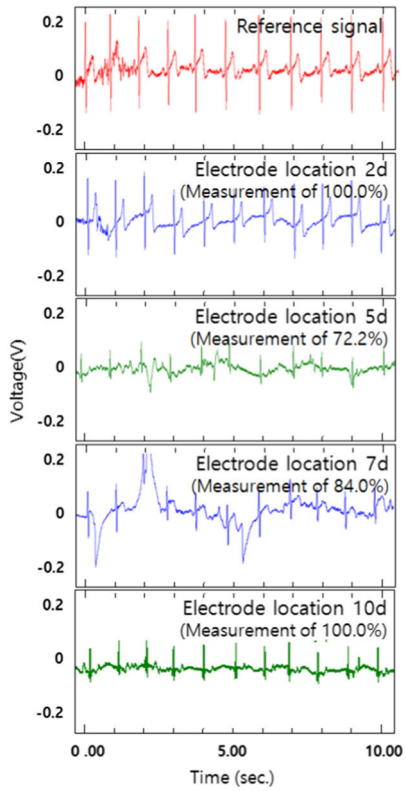

c)Horizontal plane (R)

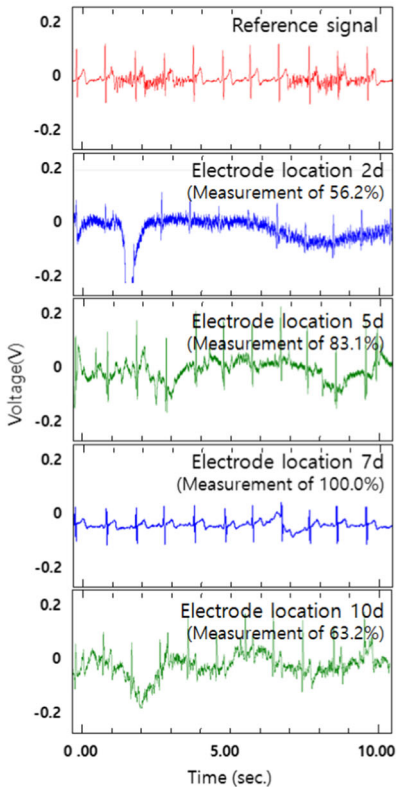

d)Frontal plane (L)

Fig. 10 Examples of ECG signal for motions of participant 5. **a** Frontal plane (R), **b**Sagittal plane (R). **c** Horizontal plane (R). **d** Frontal plane (L). **e** Sagittal plane (L). **f** Horizontal plane (L). **g** Forward flexion. **h** Backward flexion. **i** Rotation of the spine

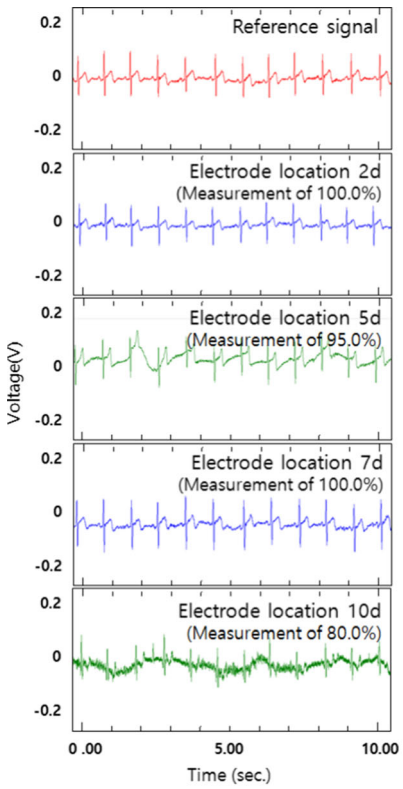

e)Sagittal plane (L)

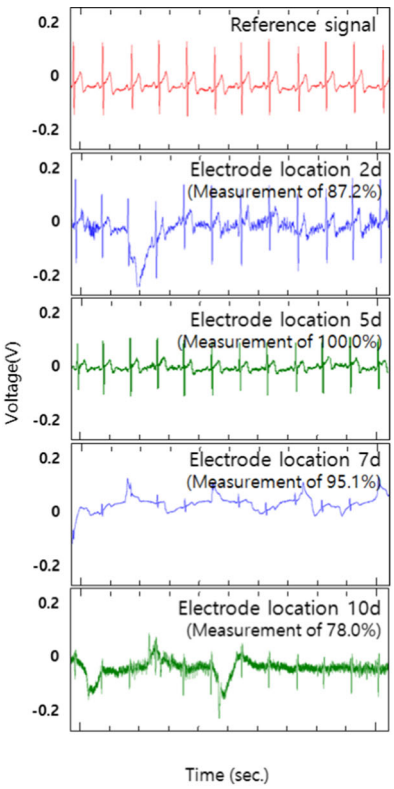

f)Horizontal plane (L)

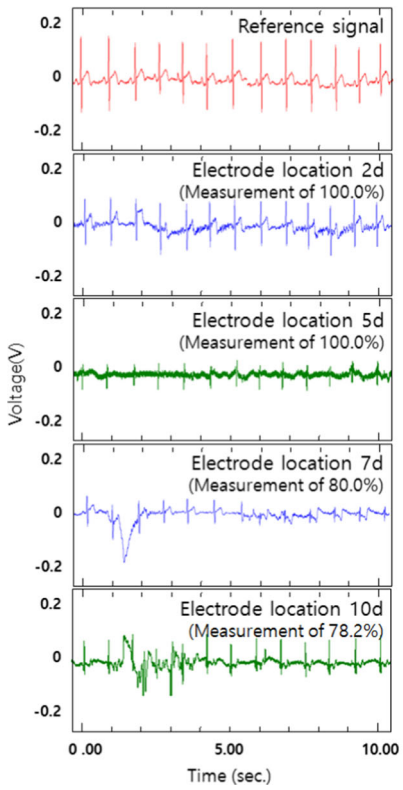

g)Forward flexion

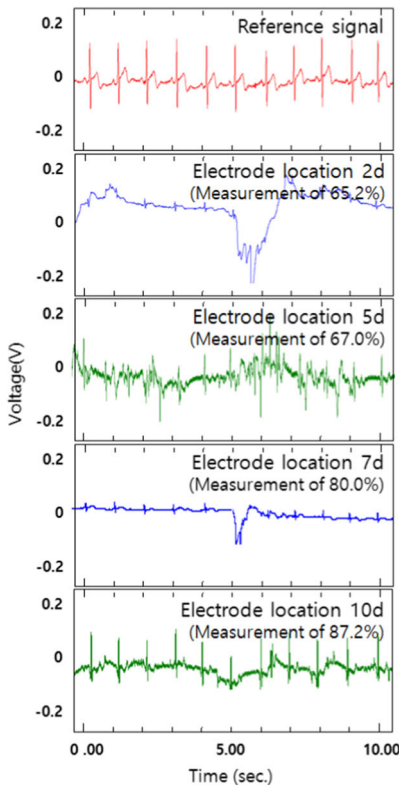

h)Backward flexion

Fig. 10 (continued)

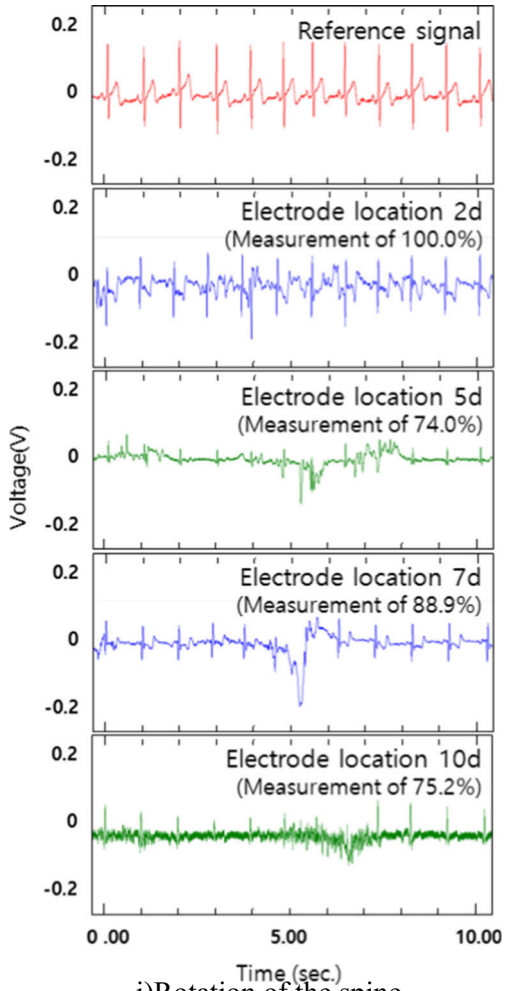

i)Rotation of the spine

Fig. 10 (continued)

(88.5 %, 0.45 V), 2e (83.9 %, 0.17 V), 3e (82.0 %, 0.11 V), 5d (91.3 %, 0.50 V), 7d (94.5 %, 0.07 V), and 10d (87.7 %, 0.12 V). Accordingly, 2c, 2d, 2e, 3e, 5d, 7d and 10d were derived as the stable electrode locations in participant 3.

In participant 4 (Fig. 9(b) and Table 2(b)), for the right arm motions, high measurement rates from 81.0 % to 97.7 % were obtained (81.0 % at electrode locations 2d, 83.0 % at 5d, 95.7 % at 9d, 97.7 % at 10c and 97.7 % at 10d). In the left arm motions, high measurement rates from 83.0 to 100.0 % were obtained (90.7 % at 5d, 86.7 % at 7c, 100.0 % at 7d, 87.0 % at 9c, 83.0 % at 10c and 83.7 % at 10d). In the bodice motions, high measurement rates were obtained at electrode locations 2d (81.0 %), 5c (95.3 %), 5d (82.3 %), 7c (81.0 %), 7d (91.3 %), 10c (83.3 %) and 10d (83.0 %). In the averaged analysis, high measurement rates and large amplitude values in the overall motions were observed at electrode locations 2d (80.4 %, 0.14 V), 5c (83.0 %, 0.17 V), 5d (84.6 %, 0.14 V), 7d (87.3 %, 0.28 V), 10c (86.8 %, 0.14 V) and 10d (86.8 %, 0.12 V). Thus, in participant 4, six positions (2d, 5c, 5d, 7d, 10c and 10d) were considered to be the stable electrode locations for ECG acquisition in the clothing.

In the case of participant 5 (Fig. 9(c) and Table 2(c)), in the right arm motions high measurement rates were observed: 87.0 % at 2d, 81.7 % at 7d, 83.3 % at 9d, 90.7 % at 10c and 88.0 % at 10d. In the left arm motions, high measurement rates were observed: 81.0 % at 2d, 81.7 % at 5c, 92.7 % at 5d, 84.0 % at 7c and 98.3 % at 7d. In the motions of the bodice, high measurement rates were observed: 96.0 % at 5c, 80.3 % at 5d, 84.0 % at 7c, 83.0 % at 7d, 86.0 % at 10c and 80.0 % at 10d. Figure 9, which presents some examples of the measured signals in the various motions at four electrode locations (2d, 5d, 7d and 10d), also affirms this in the morphological aspect. As a result, high measurement rates and a large amplitude were observed at electrode locations 2d (80.5 %, 0.16 V), 5c(81.4 %, 0.20 V), 5d (83.0 %, 0.13 V), 7d (86.5 %, 0.32 V) and 10d (80.4 %, 0.12) in participant 5.

In participant 6, in the right arm motions high measurement rates from 89.7 to 100.0 % were obtained (100.0 % at 2d, 89.7 % at 5d, 90.3 % at 7d, 98.3 % at 10c and 97.7 % at 10d). In the left arm motions, high measurement rates from 87.0 to 100.0 % were obtained (87.0 % at 2d, 80.3 % at 5c, 89.3 % at 5d, 86.7 % at 7c, 100.0 % at 7d, 89.0 % at 10c and 89.0 % at 10d). In the bodice motions, high measurement rates from 88.7 to 97.7 % were obtained (93.0 % at 2d, 97.7 % at 5c, 90.0 % at 5d, 88.7 % at 7c and 90.0 % at 10c).

In the case of participant 6, in the averaged values of the measurement rates and amplitudes across the nine motions, high measurement rates with large amplitudes were observed at 2d (93.3 % and 0.20 V), 5c (85.4 % and 0.19 V), 5d (89.6 % and 0.19 V), 7d (84.4 % and 0.34 V), 10c (91.8 %, 0.16 V) and 10d (80.2 %, 0.16 V).

In participant 7, high measurement rates were observed at electrode locations 2d (87.0 %), 5d (80.4 %), 7d (80.2 %), 9c (80.0 %), 10c (97.7 %) and 10d (97.7 %), in the right arm motions. High measurement rates were observed at electrode locations 2d (80.0 %), 5d (90.7 %), 7c (100.0 %), 7d (100.0 %), 9c (87.0 %) and 10c (83.0 %), in left arm motions. In the bodice motions, high measurement rates were observed at electrode locations 2d (96.3 %), 5c (95.3 %), 5d (82.3 %), 7c (87.0 %) and 10c (83.3 %). The average measurement rate and large amplitude values in all motions appeared to be high at 2d (89.9 %, 0.18 V), 5c(80.9 %, 0.17 V), 5d (83.9 %, 0.14 V), 7d (82.7 %, 0.13 V), 10c (86.8 %, 0.14 V) and 10d (80.1 %, 0.12 V). Accordingly, 2d, 5c, 5d, 7d, 10c and 10d were derived as the stable electrode locations in participant 7.

In the case of participant 8, in the right arm motions high measurement rates were observed: 87.0 % at 2d, 83.3 % at 9d and 90.7 % at 10d. In the left arm motions, high measurement rates were observed: 80.7 % at 2d, 81.5 % at 5c, 94.4 % at 5d, 100.0 % at 7c and 89.8 % at 7d. In the bodice motions, high measurement rates were observed at electrode locations 2d

(80.7 %), 5c (96.3 %), 5d (86.2 %), 7c (84.1 %), 7d (88.0 %) and 10c (85.9 %). In contrast, during the backward flexion motion, low measurement rates within the range of 40~70 % were observed at electrode locations 2d (60.0 %) and 5d (66.7 %), due to the larger variation caused by backward flexion than in other bodice motions. A similar trend was found in all other participants. In spite of such a contingency upon the motion type, the electrode locations of 2d and 5d appeared to be relatively stable locations for ECG measurements across the all motions.

In consideration of the averaged values of the measurement rate and amplitude across the nine motions, a high measurement rate and large amplitude of 80.1 to 82.1 % were observed at electrode locations 2d (82.3 %, 0.15 V), 5c (81.6 %, 0.20 V), 5d (86.6 %, 0.08 V), 7c (82.0 %, 0.11 V), 7d (84.3 %, 0.03 V), 10c (80.6 %,0.16 V) and 10d (81.0 %, 0.08 V).

In the case of participant 9 (Fig. 9(d) and Table 2(d)), in the right arm motions high measurement rates from 82.5 to 98.1 % were obtained (82.5 % at electrode location 1d, 98.1 % at 2c, 93.7 % at 2d, 84.3 % at 7d, 84.0 % at 8d, 92.6 %, at 9d and 86.5 % at 10d). In the left arm motions, high measurement rates from 80.7 to 100.0 % were obtained (80.7 % at electrode location 2d, 81.5 % at 5c, 94.4 % at 5d, 100.0 % at 7c and 100.0 % at 7d). In the bodice motions, high measurement rates from 81.5 to 85.0 % were obtained (85.3 % at electrode location 2d, 81.5 %, at 5c and 85.0 % at 5d). High average measurement rates and amplitude values were observed at electrode locations 2d (86.3 %, 0.18 V) and 5d (85.8 %, 0.16 V), in the lower part of the musculus pectoralis major. In the back part, the highest measurement rate and amplitude value were observed at electrode locations 7d (84.6 %, 0.09 V) and 10d (80.5 %, 0.12 V).

In participant 10, high measurement rates in the right arm motions were observed: 94.3 % at 2d, 80.0 % at 9c, 90.7 % at 10c and 97.7 % at 10d. High measurement rates in the left arm motions were observed: 90.7 % at 5d, 100.0 % at 7c, 100.0 % at 7d, 87.0 % at 9c, 83.0 % at 10c and 88.3 % at 10d. In the bodice motions, high measurement rates were observed: 96.3 % at 2d, 95.3 % at 5c, 82.3 % at 5d, 87.0 % at 7c and 83.3 % at 10d. The highest average measurement rates and largest amplitude values of participant 10 were observed at electrode location 2d (90.8 %, 0.15 V). In participant 10, in the averaged values of the measurement rate and amplitude across the nine motions, the electrode positions showing high measurement rates with large amplitudes were 2d (90.8 %, 0.32 V), 5c (80.7 %, 0.18 V), 7c (84/8 %, 0.10 V), 7d (81.7 %, 0.21 V), 10c (81.4 %, 0.12 V) and 10d (88.2 %, 0.28 V).

Generally, 2d, 5d, 7d and 10d were considered to be the most appropriate locations for the ECG measurement in a garment due to the high and stable measurement results. These locations were located under the upper musculus pectoralis major and trapezius, were least affected by muscle variation movements and exhibited stability in the measurement rate and amplitude values compared to the other electrode locations.

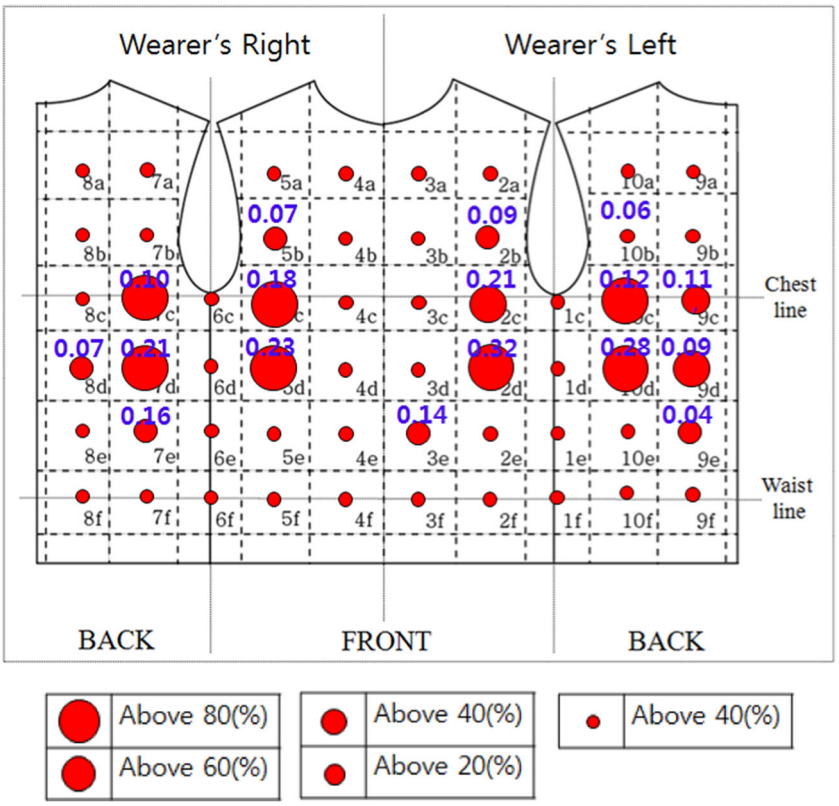

Fig. 11 Results of the average measurement rate and amplitude

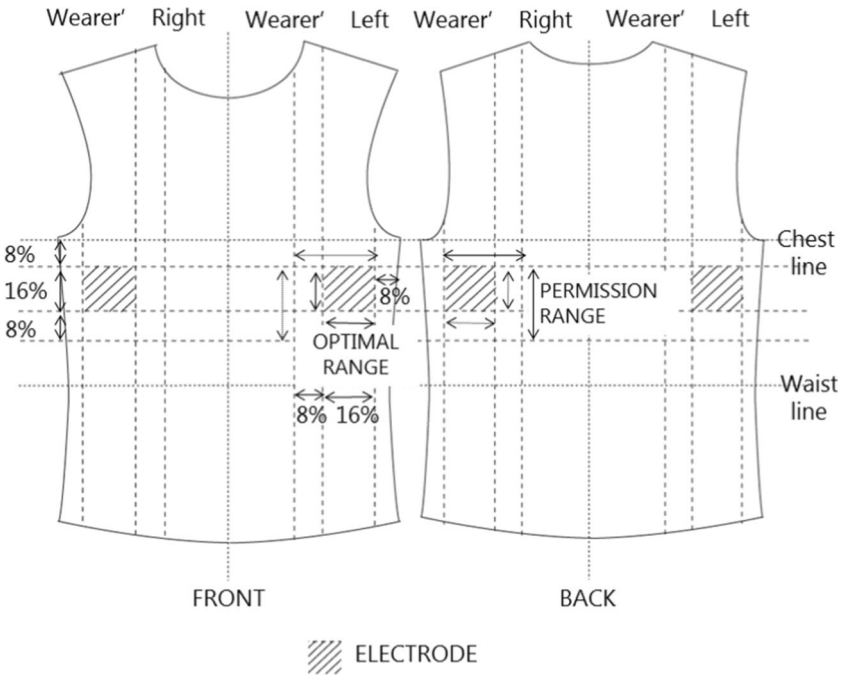

Fig. 12 A platform for garment-formed ECG monitoring

When the measurement rate for each motion was examined, measurement rates at electrode locations 2d and 5d significantly decreased in the vertical direction motions, such as in the (R) and (L) frontal plane (Fig. 10). These results imply that the measurement rate is more affected in the vertical direction than in the horizontal direction.

At electrode locations 2d and 5d in the front part, lower measurement rates were observed in the backward flexion; at electrode locations 7d and 10d in back part, lower measurement rates were observed in the forward flexion (Fig. 10). This means that the motion artifact occurred more in the skin flexion than the skin bending.

Derivation of the optimal locations of the electrode

The following shows the integrated results of what was observed in the cases of all 10 participants across the nine motions in this study.

Although the measurement rates of the ECG obtained through the electrodes on the experimental garment in the motions varied from 0 % up to 100 % depending upon the electrode location, some obviously consistent phenomena contingent upon the electrode location were discovered in this study. Although high measurement rates were observed at electrode locations 2c, 5c, 7c, and 10c in most measurement cases, the measurements in lane c were largely affected by arm movements, showing a large deviation in measurement rates since these electrodes were located above the pectoral muscle and the trapezius. In electrode location 2c, the amplitude value was high owing to the location near the heart, but the motion artifact caused by the movement of the electrode was significant. Due to this significant motion artifact, electrode location 2c was ruled out from the pool of optimal electrode locations.

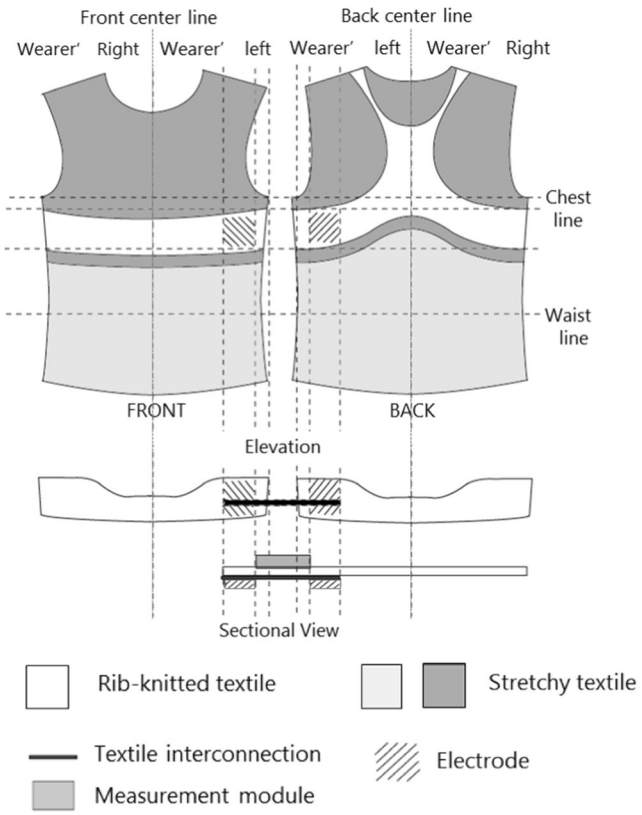

Fig. 13 Garment design B for ECG monitoring based on the optimal electrode locations

Lane ‘d’, located below the upper musculus pectoralis major and trapezius, was found to be least affected by the muscle variations in the motions by showing stability in both the measurement rate and amplitude values. In the right arm motions, high measurement rates were observed: 89.6 % at 2d, 81.4 % at 5d and 92.6 % at 10d. In the left arm motions, high measurement rates were observed: 81.3 % at 2d, 91.6 % at 5d, 89.1 % at 7c, 98.8 % at 7d and 80.5 % at 10d. In the bodice motions, high measurement rates were observed: 84.4 % at 2d, 87.7 % at 5c, 86.8 % at 5d and 80.9 % at 7d. In the averaged values of the measurement rates and amplitude across the nine motions, high measurement rates were observed: 84.9 % at 2d, 86.6 % at 5d, 84.5 % at 7d and 82.1 % at 10d. On the other hand, large amplitude values were generally observed: 0.32 at 2d, 0.23 at 5d, 0.21 at 7d and 0.28 at 10d (Fig. 11).

This indicates that four positions, 2d, 5d, 7d and 10d, were less affected by the wearer’s motions when compared with other areas. Therefore, electrode positions 2d, 5d, 7d and 10d were considered to be the optimal locations of the electrode for the ECG measurements of motions.

To summarize, 5d and 2d were found to be the optimal locations of the electrode for ECG measurements in the front part of the clothing, while 7d and 10d appeared to be the optimal sensor locations in the back part. Among all the electrode locations for the ECG measurements, 2d was found to be the most stable location in all participants.

The measurement rates higher than 80.0 % across the participant were summarized in Table 2. This measurement rates tended to be mostly obtained from the electrode positions located in lane ‘c’ and ‘d’ near to chest circumference line in horizontal direction, and in line ‘2’, ‘5’, ‘7’, ‘10’ near to the both side in vertical direction. Based on this result, ECG through the garment tended to be obtained from the specific zones in the bodice, the junction zones between the chest circumference and the both side as presented in Fig. 11.

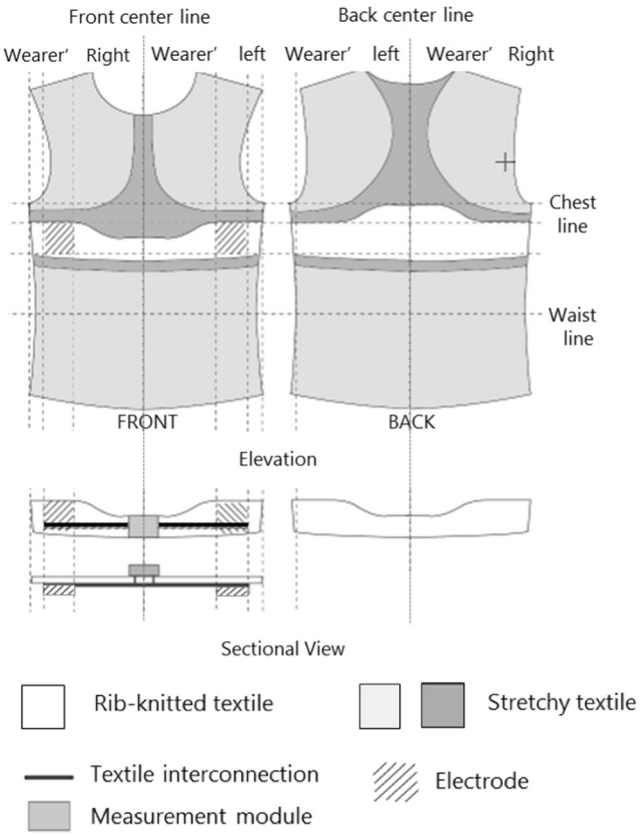

Fig. 14 Garment design B for ECG monitoring based on the optimal electrode locations

Conclusion

The aim of this study is to suggest a design for ECG–monitoring clothing that contributes to the reduction of the motion artifact. In order to implement it, this research sought to find optimal locations for electrodes on the ECG-measuring garment, which are least influenced by the motion of the human body.

This research resulted in the derivation of four optimal electrode locations in lane ‘d’ below the upper musculus pectoralis major and trapezius on the ECG-monitoring garment platform. Among the four locations, two electrode positions, 2d and 5d, were found in the lower part of both sides of the musculus pectoralis major on the front bodice, while the other two positions, 7d and 10d, were found in the lower part of both sides of the latissimus dorsi muscle on the back bodice.

From the standpoint of clothing engineering, these four electrode locations coincide with the traditionally known ‘least dynamic zone in the human bodice’ around the chest line. In addition, the signal from the left side of the musculus pectoralis major, electrode location 2d, corresponding to the position of the ‘point of maximal impulse’ (PMI) in medical science [22], showed the highest amplitude of an ECG in this study.

Based on the results of this research, a guideline for the physical electrode locations for designing the ECG-monitoring garment in various sizes is suggested in Fig. 12. An optimal electrode range is suggested by a reference point defined as the back length and breast width.

Based on the guideline in Fig. 12, two designs for the ECG-monitoring garment are presented (Figs. 13 and 14). The suggested garment is designed for tight-fitted sports shirts to attach the electrode on the body by applying a pattern cutting based on the optimal electrode location and body structure for stable signal measurements.

For design of the ECG-measurement clothing, textile materials should be positioned taking into account the degree of stretch for stable measurements and body movement. As it requires sufficient pressure for adherence to the skin, an

enhanced textile such as a rib-knitted structure is generally selected for the textile electrode part of the material. Additionally, a surrounding matrix consisting of a stretchable textile is applied in an ergonomic clothing position.

For both designs, it is assumed that a textile interconnection consisting of the conductive textile material, and a small-sized detachable hardware device including a processor, transmitter and battery are utilized. In either design, the ECG-monitoring sports shirt is configured with a combination of the 'measurement module' and the remaining parts of the garment.

In garment design A, the measurement module, including a set of the electrodes, is placed on the front and back of the left side of bodice below the chest line (Fig. 13). A hardware device is attached to the center part of the two electrodes in design A.

In garment design B, the measurement module is located only on the front chest. Among the two electrodes included in the measurement module, one electrode is located on the left side while the other one is placed on the opposite side (Fig. 14). A detachable hardware device is located in the center of the two electrodes in design B.

A future study is needed to verify the effects of the proposed garment design of ECG-monitoring clothing derived in this study. In addition, studies should include participants of various ages and body types, as well as individuals of both sexes.

Ethical standards The experiments comply with the current laws of the country in which they were performed.

Conflict of interest The authors declare that they have no conflict of interest.

References

1. Catherwood, P. A., Donnelly, N., Anderson, J., and McLaughlin, J., ECG motion artefact reduction improvements of a chest-based wireless patient monitoring system. *Comput. Cardiol.* 37:557–560, 2010.
2. Cho, H.-S., Koo, S.-M., Lee, J., Cho, H., Kang, D.-H., Song, H.-Y., Lee, J.-W., Lee, K. H., and Lee, Y.-J., Heart monitoring garment using textile electrodes for healthcare applications. *J. Med. Syst.* 35: 189–201, 2011.
3. Cömert, A., Honkala, M., and Hyttinen, J., Effect of pressure and padding on motion artifact of textile electrodes. *BioMed. Eng. Online* 2013:12–26, 2013.
4. De Rossi, D., and Veltink, P. H., Wearable technology for biomechanics: e-textile of micromechanical sensor? *IEEE Eng. Med. Biol. Mag.* 29:37–43, 2010.
5. Finlay, D. D., Nugent, C. D., Donnelly, M. P., McCullagh, P. J., and Black, N. D., Optimal electrocardiographic lead systems: practical scenarios in smart clothing and wearable health systems. *IEEE Trans. Inf. Technol. Biomed.* 12(4):433–441, 2008.
6. Fletcher, G. F., Balady, G. J., AmSterdam, e. A., Chaitman, B., Eckel, R., Fleg, J., Froelicher, V. F., Leon, A. S., I. L, Rodney, P. R., Simons-Morton, D. G., Williams, M. A., and Bazzarre, T. Exercise standards for testing and training. J. Am. Heart Assoc. 1694–1740, 2008.
7. Griffiths, A., Das, A., Fernandes, B., and Gaydecki, P., A portable system for acquiring and removing motion artefact from ECG signals. *J. Phys. Conf. Ser.* 76(1), 012038, 2007.
8. Jeong, Y., Kim, S.-H., and Yang, Y., Development of tight-fitting garments with a portable ECG monitor to measure vital signs. *J. Korean Soc. Cloth. Text.* 34(1):112–125, 2009.
9. Koo, H. R., Lee, Y.-J., Gi, S., Khang, S., Lee, J. H., Lee, J.-H., Lim, M.-G., Park, H.-J., and Lee, J.-W., The effect of textile-based inductive coil sensor positions for heart rate monitoring. *J. Med. Syst.* 38:2, 2014.
10. Kyriacou, E., Pavlopoulos, S., Berler, A., Neophytou, M., Bourka, A., Georgoulas, A., Anagnostaki, A., Karayiannis, D., Schizas, C., Pattichis, C., Andreou, A., and Koutsouris, D., Multi-purpose healthcare telemedicine systems with mobile communication link support. *BioMed. Eng. Online* 2(1):7, 2003.
11. Lee, K., and Park, H. S., A study in the perceived health status, depression and activities of daily living for the elderly in urban areas. *Korean J. Women Health Nurs.* 12(3):221–230, 2006.
12. Liu, S.-H., Motion artifact reduction in electrocardiogram using adaptive filter. *J. Med. Biol. Eng.* 31(1):67–72, 2010.
13. Mühlsteff, J., Such, O., Schmidt, R., Pekuhn, M., Reiter, H., Lauter, J., Thijs, J., Müsch, G., and Harris M., Wearable approach for continuous ECG- and activity patient-monitoring. 26th Annual International Conference of the IEEE Engineering in Medicine and Biology Society, 1(5):2184–2187, 2004
14. Pacelli, M., Loriga, G., Taccini, N., and Paradiso, R. Sensing fabrics for monitoring physiological and biomechanical variables: E-textile solutions, Medical Devices and Biosensors, 2006. International Summer School on 3rd IEEE-EMBS 1–4, 2006.
15. Pacelli, M., Paradiso, R., Anerdi, G., Ceccarini, S., Ghignoli, M., Lorussi, F., Scilingo, E. P., De Rossi, D., Gemignani, A., and Ghelarducci, B., Sensing threads and fabrics for monitoring body kinematic and vital signs. Fibres and Textiles for Future - 90th Anniversary of Academic Textile Research and Education in Finland :55–63, 2001.
16. Paradiso, R., Wearable heath care system for vital signs monitoring. 4th International. IEEE Special Topic Conference: Information Technology Applications in Biomedicine, 283–286, 2003.
17. Park, S., and Jayaraman, S., Enhancing the quality of life through wearable technology. *IEEE Eng. Med. Biol. Mag.* 22(3):41–48, 2003.
18. Shimuzu, K., Telemedicine by mobile communication. *IEEE Eng. Med. Biol. Mag.* 18(4):32–44, 1999.
19. Silva Cunha, J. P., Cunha, B., António, Xavier, W., Ferreira, N., Meireles, L., and Pereira, S. Vital-Jacket®: a wearable wireless vital signs monitor for patients' mobility in Cardiology and Sports. 2010 4th International Conference Pervasive Computing Technologies for Healthcare (PervasiveHealth) :1–2, 2010.
20. Song, H.-Y., Design of woven textile electrode for monitoring the electrical activity of the heart in smart sportswear, Ph.D. Thesis, Department of Clothig and Textiles, Yonsei University, 2010.
21. Suave Lobodzinski, S., and Laks, M. M., Comfortable textile-based electrocardiogram systems for very long-term monitoring. *Cardiol. J.* 15(5):477–480, 2008.
22. Wang, Y., Doleschel, S., Wunderlich, R., and Heinen, S., A wearable wireless ECG monitoring system with dynamic transmission power control for long-term homecare. *J. Med. Syst.* 39:35, 2015.
23. Yoon, S. W., Min, S. D., Yun, Y. H., Lee, S., and Lee, M., Adaptive motion artifacts reduction using 3-axis accelerometer in E-textile ECG measurement system. *J. Med. Syst.* 32(2):101–106, 2008.